Aerosol and Air Quality Research, 11: 860–872, 2011

ISSN: 1680-8584 print / 2071-1409 online
doi: 10.4209/aaqr.2011.08.0130

A Simplified Model of Predicting SO_2 Absorption by Single Atmospheric Raindrops with Chemical Dissociation and Internal Circulation

Wei-Hsin Chen[1*], Yuan-Yi Chen[2], Chen-I Hung[2]

[1] *Department of Greenergy, National University of Tainan, Tainan 700, Taiwan, R.O.C.*
[2] *Department of Mechanical Engineering, National Cheng Kung University, Tainan 701, Taiwan, R.O.C.*

ABSTRACT

A simplified model of predicting chemical SO_2 absorption by single freely falling raindrops with internal circulation in the atmosphere is developed in the present study. By multiplying a modification factor α into the model of interfacial velocity established from creeping flow, it is found that the relative error between the simplified model and the two-phase simulation method is less than 4%. Accordingly, the simplified model enables us to simulate the atmospheric SO_2 absorption process with less computational effort and without losing accuracy. The simulated results indicate that the dissociation of H_2SO_3 governs the mass transfer process and the concentration of HSO_3^- is by far larger than those of SO_3^{2-} and H_2SO_3. As a result, the chemical absorption takes a much longer period of time to achieve the uptake process. Specifically, for the raindrop radius in the range of 200–500 μm, the absorption time of chemical absorption is larger than that of physical absorption by the factors of 70–290. From the perspective of characteristic time, mass diffusion is the controlling mechanism for SO_2 absorption. When chemical absorption is carried out, the absorption period is 28–33 folds of the characteristic time of mass diffusion, implying that the former is always larger than the latter by over an order of magnitude.

Keywords: Raindrop; Below-cloud scavenging; Sulfur dioxide (SO_2) uptake; Transient; Chemical absorption; Model; Mass diffusion number.

INTRODUCTION

Development and utilization of energy is of the utmost importance for driving the progress of industry. Among the developed techniques of energy utilization, combustion of fossil fuels is the most commonly used route to gain heat and power or electricity. Unfortunately, when fossil fuels are burned, a number of air pollutants, such as CO, SO_x, NO_x and particulate matters, are generated and emitted into the atmosphere (Dong *et al*., 2002; Lin *et al*., 2010). In these air pollutants, sulfur dioxide (SO_2) is a noticeable one in that it will cause serious environmental damages and increase harmful risk to human health. For example, the formation of acid rain, which pertains to wet deposition, is partly due to the absorption of sulfur dioxide by atmospheric water aerosol droplets. The atmospheric water droplets widely exist in clouds, fogs and rains. When acid gases are absorbed by droplets in clouds or fogs, the in-cloud scavenging occurs (Chen, 2001a; Goncalves *et al*., 2002). Alternatively, once acid gases are absorbed by falling raindrops, the phenomenon belongs to below-cloud scavenging (Chen, 2001b; Sportisse and du Bois, 2002). Both in-cloud and below-cloud scavenging processes are the crucial mechanisms for cleaning atmosphere. In addition to the atmospheric scavenging, the two-phase transport phenomena have also been widely encountered in industrial processes for air pollution control. For instance, the basic unit of mass transfer in a wet scrubber is characterized by air pollutant uptake by droplets (Chen *et al*., 2006; Hsieh *et al*., 2011).

As far as the mechanism of formation of acid rain is concerned, it is highly relevant to the mass transfer between the gas phase and the liquid phase. In reality, the absorption processes of sulfur dioxide by raindrops are in the presence of relative motion between the drops and its environment. Once a convective flow is induced, the raindrop surface will trigger the shear stress which further elicits the internal circulation inside a raindrop (Hsu *et al*., 1994; Chen and Lu, 2003). In the past, many investigators have developed a variety of models and methods to describe the internal flow inside drops. For example, Leclair *et al*. (1972) developed four theoretical models to describe the flow patterns in the gas phase and the liquid phase. Oliver and Chung (1985, 1987) focused their attention on the flow fields inside and outside a water droplet at the Reynolds numbers less than

* Corresponding author. Tel.: 886-6-2605031;
Fax: 886-6-2602205
E-mail address: weihsinchen@gmail.com

50. Juncu (1999) highlighted the phenomena of flow for the Reynolds number up to 500 and the viscosity ratio between the gas phase and liquid phase ranging from 0.01 to 100. Yan *et al*. (2002) used a moving mesh to calculate the flows inside and outside a droplet. Bhattacharyya and Singh (2010) studied a liquid droplet falling in a continuous phase by solving the Navier-Stokes equations and the energy equation to simulate the buoyancy-assisted flow and heat transfer and the interaction between the wake flow and the heat transfer have been outlined. However, the process of solute absorption by droplets were absent in these studies.

As illustrated above, the absorption of SO_2 by an atmospheric water drop plays an vital role in the formation of acid rain. Regarding the solute absorption by moving drops, it has been discussed by a number of researchers. For example, the solute uptake in a droplet experiencing heat transfer with internal motion has been explored by Lu *et al*. (1998). In their study, the effects of internal circulation and exothermic behavior leaded to various mass transfer efficiencies. Chen (2001a; 2001b) investigated two types of scavenging, namely, the in-cloud scavenging and the below-cloud one by means of a two-phase simulation method. They addressed that the strength of internal circulation in a droplet would affect the period of absorption process. Elperin *et al*. (2005; 2007) developed a model by combining the generalized similarity transformation method and Duhamel's theorem to simulate the absorption process. In their developed model, a droplet absorbing various gases, such as SO_2, CO_2, H_2S, Cl_2 and HCl, at altered Peclet numbers has been examined, and the absorption processes at various altitudes in the air were reported. Considering the effect of Reynolds number and Peclet number with emphasis on large value of Peclet number, Juncu (2010) investigated the unsteady heat and mass transfer inside a circulating fluid sphere.

Despite numerous studies concerning droplet internal motion and mass transfer between the gas phase and the droplet phase conducted, the review of past works suggests that relatively little research has been performed on SO_2 absorbed by raindrops under the combining effect of chemical reaction and internal circulation in the drops. In fact, when SO_2 is scavenged by a raindrop, chemical reactions will occur in the liquid phase. Specifically, following the formation of sulfurous acid ($SO_2 \cdot H_2O$) from sulfur dioxide (SO_2), it will dissociate into hydrogen sulfite (HSO_3^-), sulfite ion (SO_3^{2-}) and hydrogen ion (H^+), and these reactions will enhance SO_2 uptake from the gas phase. Detailed coupling phenomena from the chemical reactions and drop internal motion are still insufficient so far. For this reason, one of the purposes of this study is to explore the SO_2 absorption processes in freely falling raindrops at various drop sizes or terminal velocities. On the other hand, the interfacial velocity distribution along a moving droplet surface has been established by Leclair *et al*. (1972). However, their model was subject to the condition of creeping flow. In the present study, a simplified model accounting for the interfacial velocities of falling raindrops will be developed. With the developed model, only the liquid phase is required to be solved, thereby reducing the computational procedure from the two-phase simulation.

MATHEMATICAL FORMULATION

Physical Description and Governing Equations

Sulfur dioxide uptake by a freely falling raindrop with terminal velocity serves as the basis of the present study to figure out the chemical absorption dynamics inside the raindrop. When a raindrop falls in the air, a relative motion between the gas phase and the liquid phase will trigger an internal motion inside the raindrop. Considering SO_2 uptake, the processes are related to physical gas dissolution and chemical dissociations (Seinfeld, 1986) and they are expressed in Table 1. In the entire absorption processes, some assumptions are adopted to simplify the physical problem. They include: (1) the shape of the raindrop remains spherical; (2) the fluids are Newtonian as well as the flows are isothermal, incompressible and axisymmetric along the centerline of the drop; (3) mass transport takes place in the drop alone because of low mass diffusion number (Chen, 2002); (4) phase equilibrium prevails at the drop surface and gas dissolution obeys Henry's law; (5) aqueous mass diffusion abides by Fick's law; (6) the diffusivities of all species in the drop are equivalent; and (7) the properties of fluids are constant.

Governing Equations as well as Initial and Boundary Conditions

The governing equations consist of the continuity, momentum and species equations and they are shown in Fig 1. The subscript i shown in the species equations represents $SO_2 \cdot H_2O$, HSO_3^-, SO_3^{2-} or H^+. The reaction source terms, R_i, are expressed in terms of the forward reactions and the equilibrium constants (Chen *et al*., 2009) and they are written in Table 1 as well. In the table, k_f and K_{eq} are the forward reaction rate constant and the equilibrium constant, respectively. The equilibrium constants are also given in Table 1. According to thermodynamics (Sonntag, 1994) the equilibrium constant of reaction r is expressed as:

$$K_{eq,\,\mathrm{r}} = \exp\left[\sum_{i=1}\left(\nu''_{i,r}-\nu'_{i,r}\right)\frac{s_i^0}{R}-\sum_{i=1}\left(\nu''_{i,r}-\nu'_{i,r}\right)\frac{h_i^0}{R}\right]\left(\frac{p_{atm}}{RT}\right)^{\sum_{i=1}\left(\nu''_{i,r}-\nu'_{i,r}\right)} \quad (1)$$

In the preceding equation, $\nu'_{i,\,r}$ and $\nu''_{i,\,r}$ are the stoichiometric coefficients for the reactant and product i in the reaction r; s_i^0, h_i^0, R, p_{atm} and T are the standard-state entropy (J/kgmol-K), standard-state enthalpy (J/kgmol), universal gas constant (= 8314.32 J/kgmol-K), atmospheric pressure (= 101325 Pa) and temperature (K), respectively. The values of s_i^0, h_i^0, $k_{f,i}$ and $K_{eq,i}$ are given in Table 2.

In this study, it is assumed that at a certain moment SO_2 is absorbed by a raindrop with terminal velocity, that is, the onset of SO_2 uptake occurs at t = 0. The initial and boundary conditions are expressed in Fig. 1 as well. In the study of Leclair *et al*. (1972), the velocity distribution along a drop surface with creeping flow ($Re_g \leq 1$) was modeled by

Table 1. A list of physical dissolution and chemical dissociation for SO_2 absorbed by a water droplet, chemical reaction rate and equilibrium constant.

Equation	Reaction rate	Equilibrium constant
$SO_{2(g)} + H_2O_{(l)} \leftrightarrow SO_2 \cdot H_2O_{(aq)}$	$R_{SO_2 \cdot H_2O} = k_{f,\,SO_2 \cdot H_2O}\left(C_{SO_2 \cdot H_2O} - \frac{1}{K_{eq,\,SO_2 \cdot H_2O}} C_{HSO_3^-} C_{H^+}\right)$	$K_{eq,\,SO_2 \cdot H_2O} = \frac{C_{HSO_3^-,\,eq} \cdot C_{H^+,\,eq}}{C_{SO_2 \cdot H_2O,\,eq}}$
$SO_2 \cdot H_2O_{(aq)} \leftrightarrow HSO_{3(aq)}^- + H_{(aq)}^+$	$R_{HSO_3^-} = k_{f,\,HSO_3^-}\left(C_{HSO_3^-} - \frac{1}{K_{eq,\,HSO_3^-}} C_{SO_3^{2-}} C_{H^+}\right)$	$K_{eq,\,HSO_3^-} = \frac{C_{SO_3^{2-},\,eq} \cdot C_{H^+,\,eq}}{C_{HSO_3^-,\,eq}}$
$HSO_{3(aq)}^- \leftrightarrow SO_{3\,(aq)}^{2-} + H_{(aq)}^+$		
$H_2O_{(l)} \leftrightarrow H_{(aq)}^+ + OH_{(aq)}^-$	$R_{H_2O} = k_{f,\,H_2O}\left(C_{H_2O} - \frac{1}{K_{eq,\,H_2O}} C_{OH^-} C_{H^+}\right)$	$K_{eq,\,H_2O} = \frac{C_{OH^-,\,eq} \cdot C_{H^+,\,eq}}{C_{H_2O,\,eq}}$

$$V_\theta = \frac{1}{2}\frac{\mu_g}{\mu_l} U_\infty \sin\theta \tag{2}$$

With the foregoing model, the flow field inside the drop is characterized by Hill's vortex structure (Sirignano, 1999) and it is proper to consider the flow field in the drop alone. However, when the Reynolds number is large to a certain extent, the velocity profile departs from the sinusoidal distribution, stemming from the difficulty of pressure recovery at the aft region of the drop. Under such a situation, Eq. (2) is inappropriate to describe the drop surface velocity. To overcome the aforementioned restriction, a simplified model accounting for the effect of higher Reynolds number is developed by multiplying a modification factor on the model of Leclair *et al*. (1972) and the factor is a function of Reynolds number.

Numerical Method and Physical Scale

To solve the governing equations in association with the initial and boundary conditions, the commercial software ANSYS FLUENT v12 was utilized. In the software, the finite volume method (Patankar, 1980) was employed to discretize the equations shown in Fig. 1. Afterward, the SIMPLE algorithm was followed to approach the solutions of the equations. In the course of calculation, the first order upwind scheme was used. As far as the grid system is concerned, an orthogonal grid system of 49 × 81 ($r \times \theta$) was adopted. From the tests of a number of grid systems, it was found that the adopted grid system satisfied the requirement of grid independence.

When the absorption process is investigated, a number of parameters, such as the dimensionless SO_2 absorption amount ($m'_{SO_2 \cdot H_2O}$), dimensionless species concentration (C_i'), local Sherwood number (Sh_θ) and mean pH value, are taken into account. These parameters are expressed as follows.

$$m'_{SO_2 \cdot H_2O} = \frac{3}{2}\int_0^1 \int_0^\pi \frac{C_{SO_2 \cdot H_2O}}{H_{SO_2} p_{SO_2}} r'^2 \sin\theta \, d\theta \, dr' \tag{3}$$

$$C_i' = \frac{C_i}{H_{SO_2} p_{SO_2}} \tag{4}$$

$$Sh_\theta = \frac{\partial}{\partial r'}\left(\frac{C_{SO_2 \cdot H_2O}}{H_{SO_2} p_{SO_2}}\right) \tag{5}$$

$$\mathrm{PH} = -\log\left(\frac{3}{2}\int_0^1 \int_0^\pi C_{H^+} r'^2 \sin\theta \, d\theta \, dr'\right) \tag{6}$$

where r' ($= r / r_s$) is the dimensionless radial coordinate. Meanwhile, the dimensionless absorption rate is defined as

$$\dot{m}'_{SO_2 \cdot H_2O} = \frac{m'_{SO_2 \cdot H_2O,\,qss}\, r'}{t'_{qss}} \tag{7}$$

where $t'_{qss}(=t_{qss}/t_{qss,\,\mathrm{PA},\,r_s=200\,\mu m})$ is the dimensionless quasi-saturated time.

RESULTS AND DISCUSSION

In the present study, attention is paid to SO_2 absorption by freely falling raindrops in the atmosphere with room temperature (298 K). Four different drop radii of 200, 300, 400 and 500 μm are investigated. Detailed values of fluid properties (air and water), aqueous mass diffusivity and Henry's law constant are tabulated in Table 3. Meanwhile, corresponding to the aforementioned radii, the values of terminal velocity of the raindrops, mean drop surface velocity and Reynolds number are provided in the table as well. In general, the SO_2 concentration in the atmosphere is in the range of 0.1 ppb–0.2 ppm (Seinfeld, 1986), and it is typically around 0.01 ppm in Taiwan; the preceding value is thus adopted in the current study. In the following section, the velocity distributions and absorption processes from the simplified model (SM) and the two-phase simulation method (TPSM) will be compared with each other.

Modeling of Surface Velocity

From Table 3 it can be found that the drop Reynolds number is in the range of 41–250 which substantially departs from the creeping flow. Therefore, the velocity distribution developed by Leclair *et al*. (1972) is modified by the following equation

$$V_\theta = \alpha \frac{1}{2}\frac{\mu_g}{\mu_l} U_\infty \sin\theta \tag{8}$$

where α is the modification factor which is a function of Reynolds number. Fig. 2(a) first displays the values of α at the four different Reynolds numbers. Subsequently, from the plot of ln(α) versus Reynolds, it is found that a linear correlation with $R^2 = 0.994$ is clearly exhibited. Accordingly, from the slope and intercept of the regression line, the values of α can be correlated by an exponential function, that is

$$\alpha = \exp\left(5.713\times10^{-3}\,\mathrm{Re}_g + 0.7816\right) \tag{9}$$

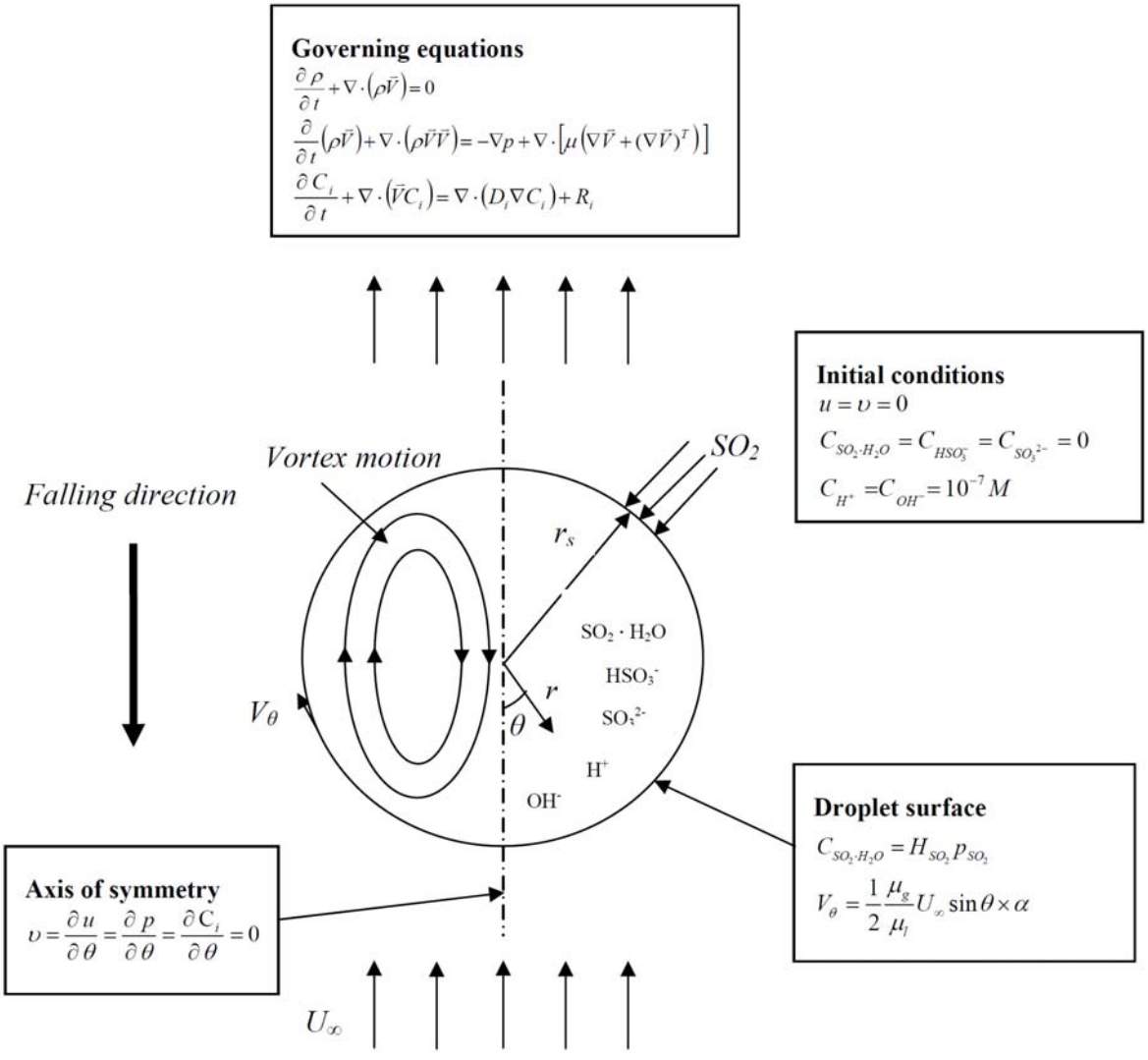

Fig. 1. A schematic of coordinate system and illustration of sulfur dioxide absorbed by an raindrop.

Table 2. Values of standard-state enthalpy h^0, standard-state entropy S^0, rate constant of forward reaction k_f and equilibrium constant K_{eq} (Schwartz and Freiberg, 1981a; Sonntag *et al*., 1994; Tanaka, 2010).

Species	h^0 (J/kgmol)	S^0 (Jkgmol-K)
$SO_2 \cdot H_2O$	–608522820	232101
HSO_3^-	–631983840	119605.2
SO_3^{2-}	–637336800	–34710.6
H^+	–14372363.88	–21328.2
OH^-	–164721800	172356.3
Reaction	k_f (1/s)	K_{eq} (M)
$SO_2 \cdot H_2O_{(aq)} \leftrightarrow HSO_{3(aq)}^- + H^+_{(aq)}$	3.4×10^6	1.61×10^{-2}
$HSO_{3(aq)}^- \leftrightarrow SO_{3(aq)}^{2-} + H^+_{(aq)}$	2.217×10^3	7.39×10^{-8}
$H_2O_{(aq)} \leftrightarrow OH^-_{(aq)} + H^+_{(aq)}$	2×10^{-5}	1.802×10^{-16}

Table 3. Values of fluid properties, aqueous mass diffusivity, Henry's law constant, temperature, the concentration of SO_2 in the gas phase, mean droplet surface velocity and Reynolds number in terms of gas properties (Schwartz and Freiberg, 1981b; Seinfeld, 1986; Mott, 1994; Chen, 2001a; Chen, 2001b).

Denotation	Value
ρ_g (kg/m^3)	1.184
ρ_l (kg/m^3)	997
μ_g (Pa s)	1.84×10^{-5}
μ_l (Pa s)	8.91×10^{-4}
D_l (m^2/s)	1.8×10^{-9}
H (M/atm)	1.26

T (K)	$C_{SO_2,\infty}$ (ppm)	r_s (μm)	U_∞ (m/s)	$\overline{V}_\theta$ (m/s)	$\mathrm{Re}_g = \frac{2\rho_g U_\infty r_s}{\mu_g}$
298	0.01	200	1.61	0.02195	41.38
		300	2.42	0.02873	93.44
		400	3.05	0.03606	137.41
		500	3.86	0.06411	248.61

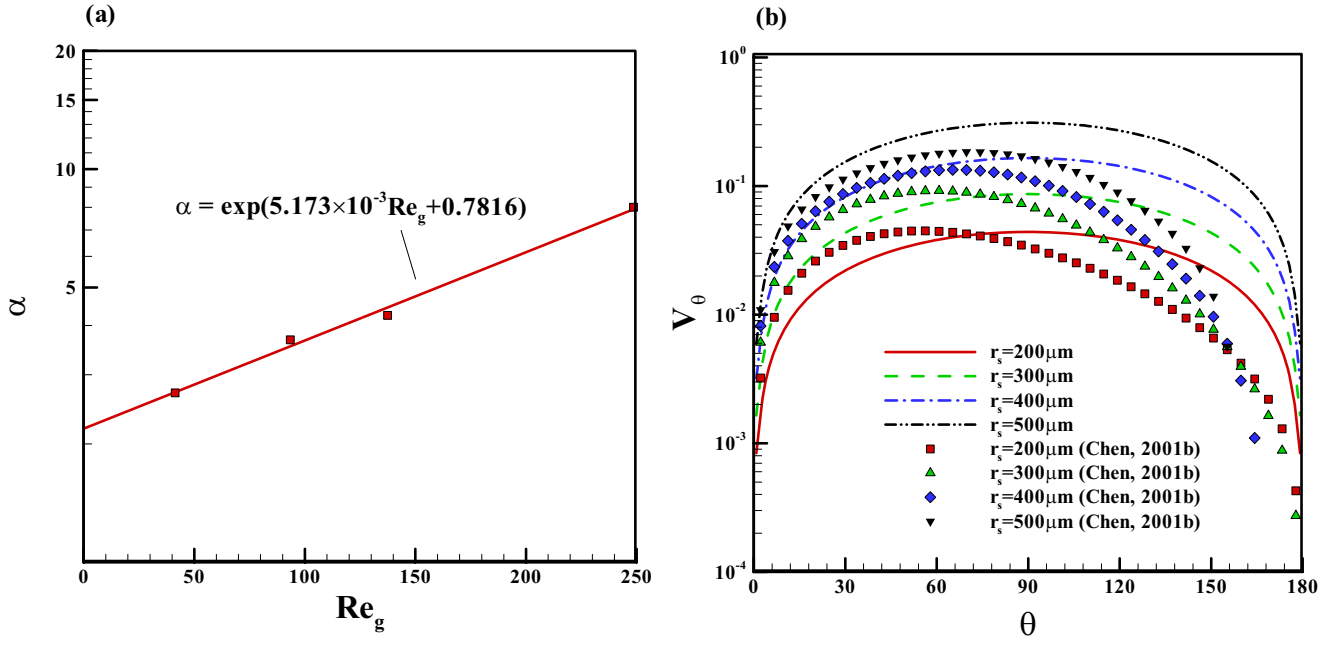

Fig. 2. The distributions of (a) modification factor and (b) tangential velocity along a raindrop surface at various drop radii.

Based on the preceding correlation, the velocity profiles between the SM (i.e. the single-phase simulation method) and the TPSM (Chen, 2001b) are compared with each other in Fig. 2(b). For the cases of 200, 300 and 400 μm, it can be seen that the velocity from the SM is overestimated at the front portion of the drop surface, whereas it is underestimated at the rear portion. This arises from the sinusoidal velocity distribution assumed in the SM which ignores the difficulty in the pressure recovery at the aft region of the raindrop. Fig. 3 presents the transient SO_2 absorption processes at various raindrop radii where only the physical absorption process is taken into account. Despite the difference in velocity distribution between the SM and the TPSM, Fig. 3(a) depicts that the absorption processes can be predicted well from the former in that the results from the SM are close to those from the TPSM. To provide a more precise comparison, the profiles of the quasi-saturated time (QST) from the two different methods and the relative error are plotted in Fig. 3(b) where the QST is identified at the moment when the dimensionless SO_2 absorption amount reaches 0.99. It is clear that the difference of QST between the SM and the TPSM are slight. The relative error between the two methods is defined as

$$\text{Relative error (\%)} = \frac{\left| t_{qss,\text{SM}} - t_{qss,\text{TPSM}} \right|}{t_{qss,\text{TPSM}}} \times 100 \qquad (10)$$

Fig. 3(b) indicates that, within the investigated range of drop radius (i.e. 200–500 μm), the relative error is less than 4%, revealing that the developed SM is able to predict the absorption process accurately.

Chemical Absorption Dynamics

Subsequently, temporal distributions of dimensionless $SO_2 \cdot H_2O$ accumulation amount at various drop radii are shown in Fig. 4 where chemical dissociations inside raindrops have been considered. To provide a detailed illustration upon the mass transfer process, a number of mathematical characteristic times are listed in Table 4, whereas the physical characteristic times corresponding to the four different raindrop radii are given in Table 5. As can be seen in Table 5, the characteristic time of mass diffusion is much longer than the others, implying that the mass diffusion is the controlling mechanism in determining the absorption process. For this reason, increasing drop radius substantially elongates the absorption process, mainly resulting from the enlargement in the distance from the drop surface to the vortex center. To proceed farther into the recognition of mass transfer, the concentration uniformity inside the raindrops are examined in Fig. 5 where the concentration uniformity is defined as

$$\Delta C'_{SO_2 \cdot H_2O} = \frac{C_{SO_2 \cdot H_2O,s} - C_{SO_2 \cdot H_2O,\min}}{C_{SO_2 \cdot H_2O,\text{s}}} \qquad (11)$$

The subscripts *s* and *min* denote the raindrop surface and the minimum, respectively. Upon the inspection of the distributions shown in Figs. 4 and 5, it can be figured out that the absorption process is subject to the concentration distribution in the raindrop. Moreover, for the raindrop with r_s = 500 μm, the figures reveal that it will take over 600s for the raindrop reaching the saturated state.

Furthermore, temporal concentration distributions of all species inside the raindrops with r_s = 200 and 500 μm are sketched in Figs. 6(a) and 6(b), respectively, where the physical absorption and chemical absorption processes are simultaneously taken into account. Again, the curves suggest that the period of achieving chemical absorption is much longer than physical one. This can be explained by chemical

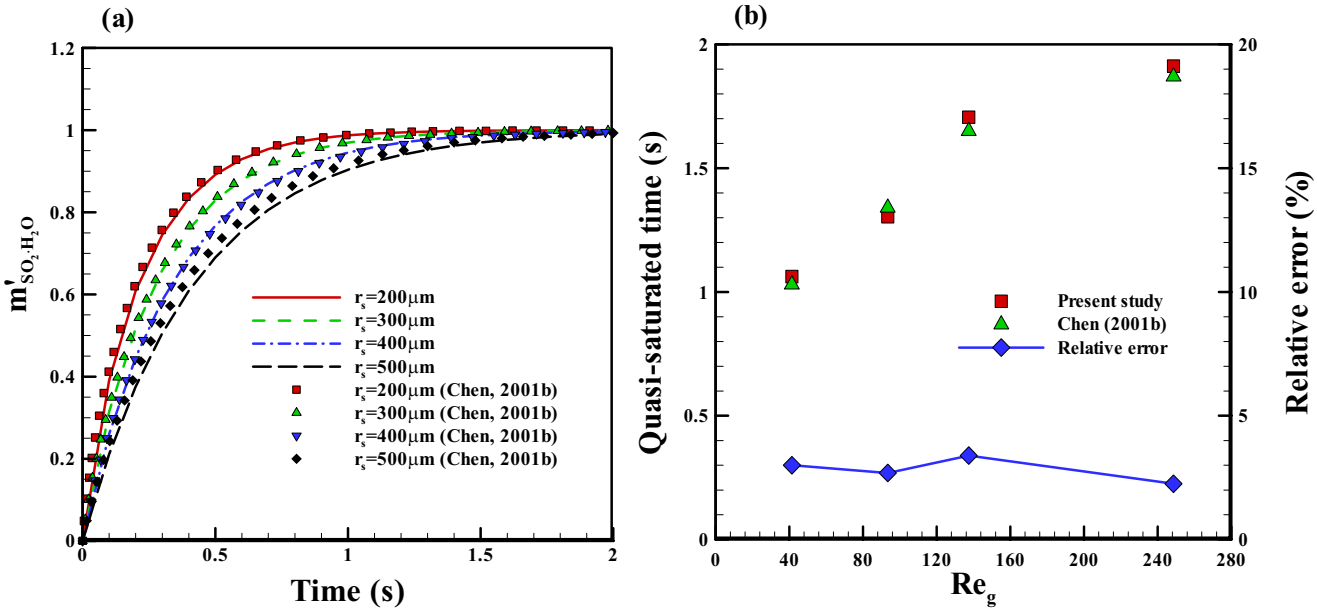

Fig. 3. (a) Transient distributions of dimensionless $SO_2 \cdot H_2O$ accumulation amount at various drop radii and (b) a comparison of quasi-saturated time between SM and TPSM at various Reynolds numbers.

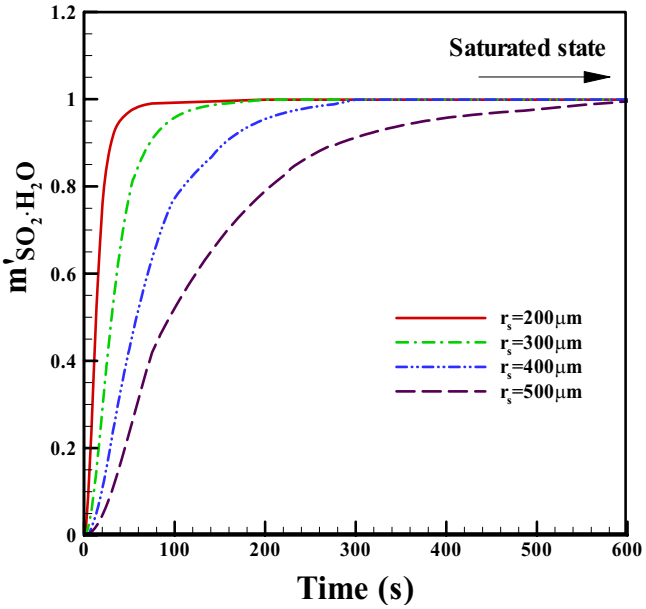

Fig. 4. Transient distributions of dimensionless $SO_2{\cdot}H_2O$ accumulation amount at various drop radii with chemical dissociations.

reactions facilitating SO_2 uptake amount of raindrops in a significant way. Table 5 has revealed that the characteristic times of phase equilibrium and chemical reactions are in the orders of 10^{-10} and 10^{-7} s, respectively, which are much shorter than those of internal circulation and mass diffusion. This implies that soon after SO_2 is absorbed by raindrops, it transforms to $SO_2{\cdot}H_2O$ followed by dissociating into HSO_3^-, SO_3^{2-} and H^+. The concentration of S(IV) is the summation of $SO_2{\cdot}H_2O$, HSO_3^- and SO_3^{2-} which is close to those of HSO_3^- and H^+. Meanwhile, the equilibrium constant of $SO_2{\cdot}H_2O$ dissociation is much larger than that of HSO_3^- dissociation so that the concentrations of HSO_3^- and H^+ is very high compared to those of $SO_2{\cdot}H_2O$ and SO_3^{2-}. Specifically, the concentrations of HSO_3^- and S(IV) are larger than that of $SO_2{\cdot}H_2O$ by a factor of over two orders in that the steady-state concentrations of the formers are around 350 whereas the concentration of the latter is 0.99, as shown in Fig. 6. Seeing that most of the SO_2 absorbed by raindrops is transformed to HSO_3^-, this results in that the SO_2 uptake amount by raindrops is governed by the dissociation of $SO_2{\cdot}H_2O$ or the formation of HSO_3^-. This is the reason that the duration of chemical absorption is fairly long compared to that of physical absorption.

Table 4. The definition of the involving characteristic times (Schwartz and Freiberg, 1981a; Seinfeld, 1986; Chen, 2001a).

Definition of characteristic time	
Convection	$\tau_c = \dfrac{r_s}{U_\infty}$
Internal circulation	$\tau_{internal\ circulation} = \dfrac{2r_s}{\bar{V}_\theta}$
Vortex formation	$\tau_{vortex\ formation} = \dfrac{r_s^2 \rho_l}{\mu_l}$
Diffusion	$\tau_d = \dfrac{r_s^2}{9D_l}$
Phase equilibrium	$\tau_p = 2\pi MRTD_l H^2$
$SO_2{\cdot}H_2O$ dissociation	$\tau_{r,\,SO_2\cdot H_2O} = \left[k_{f,\,SO_2\cdot H_2O} + \dfrac{k_{f,\,SO_2\cdot H_2O}}{K_{eq,\,SO_2\cdot H_2O}} \left(C_{eq,H^+} + C_{eq,HSO_3^-} \right) \right]^{-1}$
HSO_3^- dissociation	$\tau_{r,\,HSO_3^-} = \left[k_{f,\,HSO_3^-} + \dfrac{k_{f,\,HSO_3^-}}{K_{eq,\,HSO_3^-}} \left(C_{eq,H^+} + C_{eq,SO_3^{2-}} \right) \right]^{-1}$
H_2O dissociation	$\tau_{r,\,H_2O} = \left[k_{f,\,H_2O} + \dfrac{k_{f,\,H_2O}}{K_{eq,\,H_2O}} \left(C_{eq,H^+} + C_{eq,OH^-} \right) \right]^{-1}$

Table 5. A list of involved characteristic times (Schwartz and Freiberg, 1981a; Seinfeld, 1986; Chen, 2001a).

r_s (μm)	U_∞ (m/s)	Characteristic time (s)							
		Convection	Internal circulation	Vortex formation	Diffusion	Phase equilibrium	$SO_2{\cdot}H_2O$ dissociation	HSO_3^- dissociation	H_2O dissociation
200	1.61	1.242×10^{-4}	0.01822	0.04476	2.469	1.536×10^{-10}	2.925×10^{-7}	7.372×10^{-7}	2.017×10^{-7}
300	2.42	1.239×10^{-4}	0.02088	0.1007	5.556				
400	3.05	1.311×10^{-4}	0.02219	0.179	9.877				
500	3.86	1.295×10^{-4}	0.01559	0.2797	15.432				

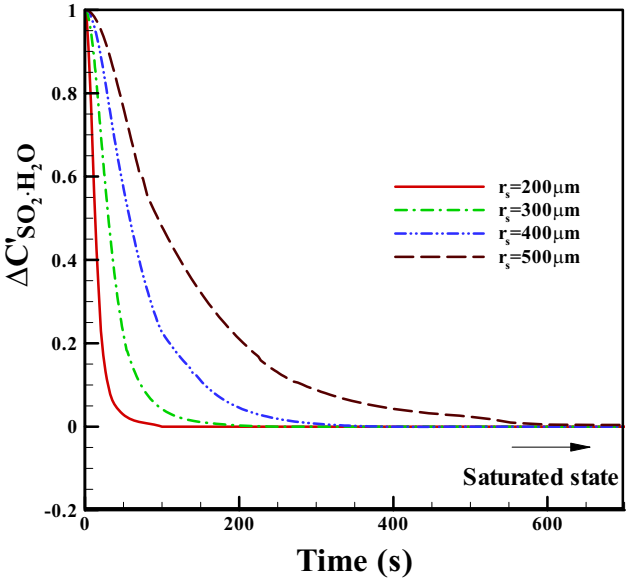

Fig. 5. Transient distributions of dimensionless concentration uniformity of $SO_2 \cdot H_2O$ in raindrops with chemical dissociations at various drop radii.

Three-dimensional (i.e. temporal and spatial) distributions of $SO_2 \cdot H_2O$, HSO_3^-, H^+ and S(IV) at the drop surface are further examined in Fig. 7. As can been seen in Table 5, the characteristic time of internal circulation is in the order of 10^{-2} s, whereas it is around 2–15 s for mass diffusion, implying that the former is smaller than the latter by two orders. In view of this difference, the interfacial concentration distributions of the four species are uniform over the entire absorption period. In contrast, there is a drastic growth in the temporal concentrations of HSO_3^-, H^+ and S(IV) for the raindrop of 200 μm within 20 s (Fig. 7(a)); they also rise markedly for the raindrop of 500 μm within the absorption time of 200s (Fig. 7(b)).

The concentration contours of HSO_3^- and SO_3^{2-} inside the raindrops of 200 and 500 μm at the absorption times of 3 and 15 s are examined in Fig. 8. Table 5 illustrates that the characteristic times of chemical reactions are in the order of 10^{-7} s which are much shorter than those of internal circulation and mass diffusion. Meanwhile, it has been recognized that mass transfer is controlled by diffusion along the streamlines toward the vortex core. For these reasons, it is not surprising that the concentration contours behave as vortex structure. For the raindrop of 200 μm, it can be observed that the concentrations of HSO_3^- at the vortex core are approximately larger than those of SO_3^{2-} by a factor of two orders (Figs. 8(a) and 8(b)). Similar results are also obtained for the raindrop of 500 μm (Figs. 8(c) and 8(d)).

Temporal distributions of mean pH value inside raindrops with various radii are presented in Fig. 9. Fig. 4 has suggested that a raindrop with smaller radius reaches the saturated state faster. Consequently, as shown in Fig. 9, the mean pH value drops faster for a smaller raindrop. Once a raindrop reaches the saturated state, the final pH value is 4.35, regardless of what size of the raindrop is. The distributions of local Sherwood number (i.e. Sh_θ) at three different absorption times are shown in Fig. 10 where the physical and chemical absorption processes are considered to account for their difference. In contrast to physical absorption, chemical dissociations cause a larger concentration gradient of $SO_2 \cdot H_2O$ at the drop surface. Therefore, the curves with chemical absorption are much higher than those with physical absorption, especially at the time of 0.1QST. In the physical absorption, the interfacial mass transfer is affected by the internal circulation to a certain extent; it is thus noted that the distributions of local Sherwood number at 0.1QST and the half-saturated time (HST), the absorption time at $m'_{SO_2 \cdot H_2O} = 0.5$, decrease with increasing polar angle. Unlike the physical absorption, the chemical dissociations are so rapid (Table 5) that SO_2 uptake is dominated by HSO_3^- dissociation. As a result, the local

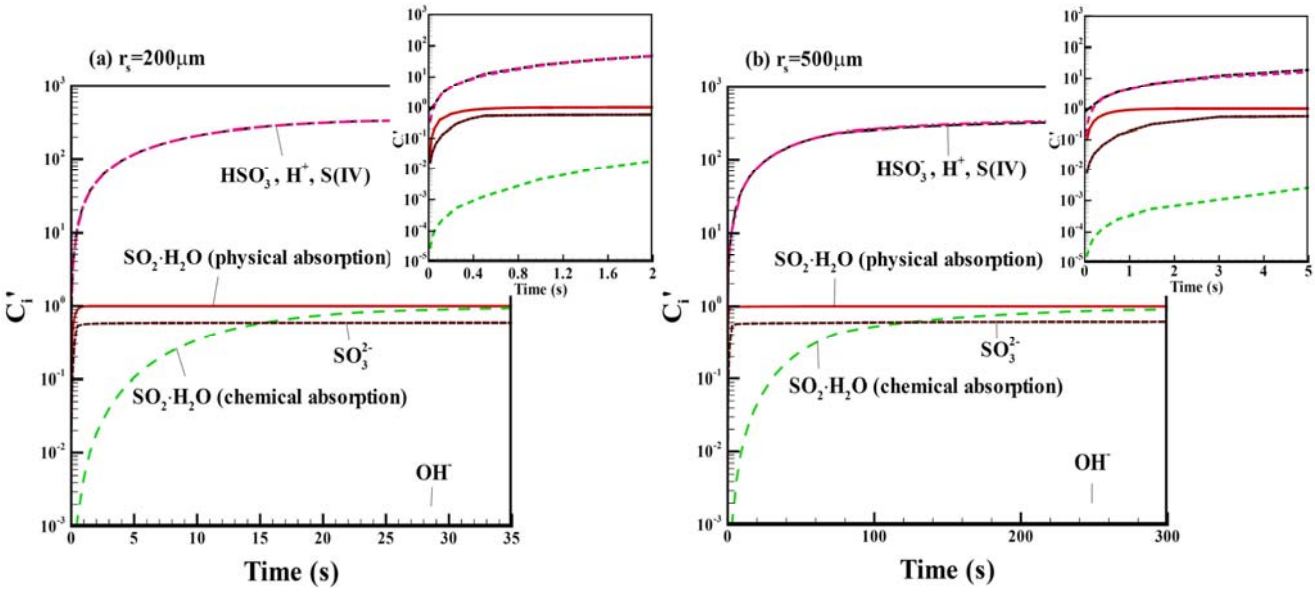

Fig. 6. Temporal concentration distributions of all species in raindrops with the radii of (a) 200 and (b) 500 μm.

Sherwood number is characterized by a horizontal distribution. Once the absorption time reaches QST, almost no SO_2 is absorbed by raindrops, rendering that the curves are close to zero.

Absorption Period and Rate

To provide a deep insight into the difference between the physical and chemical absorptions, their profiles of QST are compared with each other in Fig. 11(a). When the Reynolds

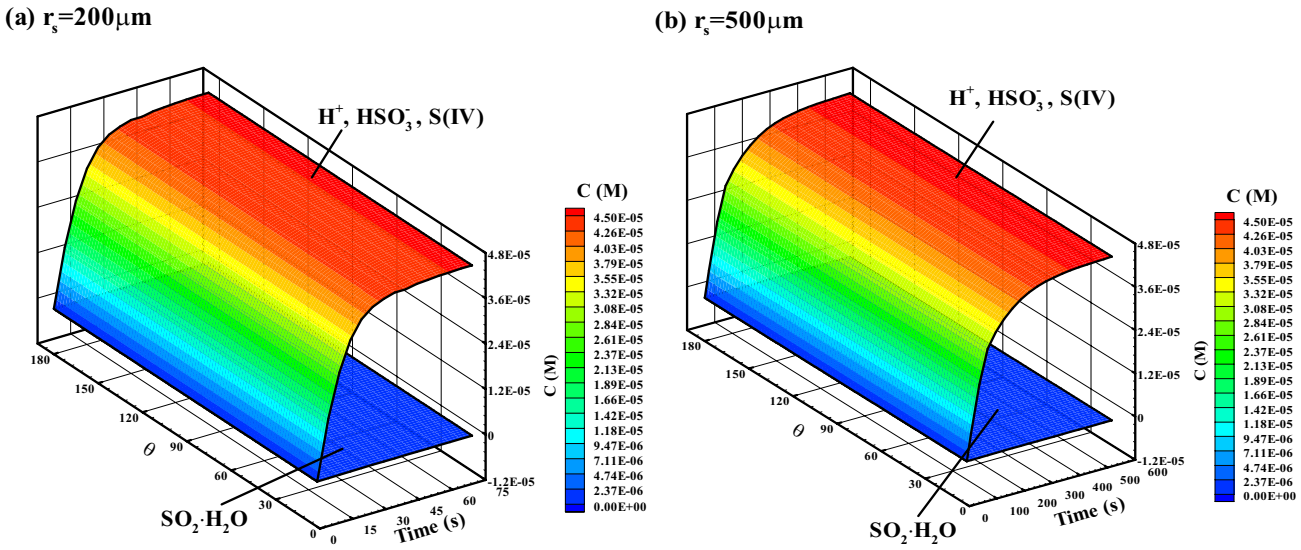

Fig. 7. Spatial and temporal distributions of species concentrations along the raindrop surface at r_s= (a) 200 and (b) 500 μm.

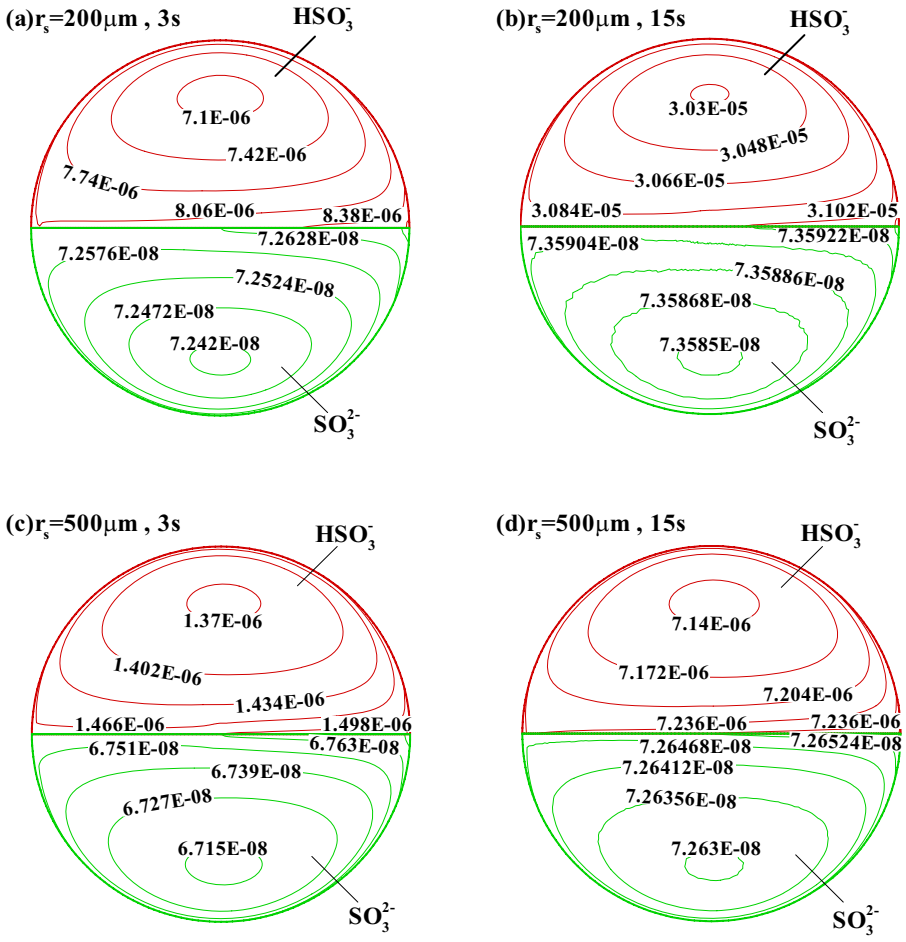

Fig. 8. Concentration contours of HSO_3^- and SO_3^{2-} in raindrops with r_s = 200 μm at the absorption times of (a) 3 and (b) 15 s as well as with r_s = 500 μm at the absorption times of (c) 3 and (d) 15 s.

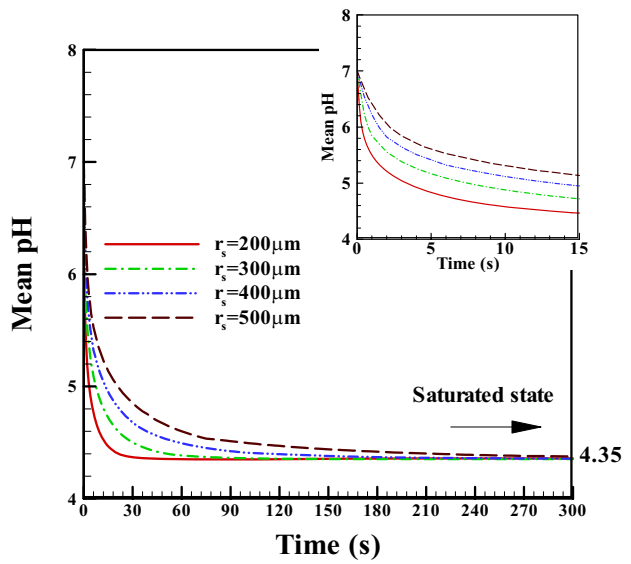

Fig. 9. Temporal distributions of mean pH value inside raindrops at various drop radii.

number or raindrop size increases, the QST increases as well, regardless of the physical absorption and chemical absorption considered. Corresponding to the drop radii of 200, 300, 400 and 500 μm, the values of QST from the physical absorption are 1.06, 1.30, 1.70 and 1.91 s, respectively, whereas they are 75, 155, 284 and 552 s, respectively, for the chemical absorption. Accordingly, the ratio of chemical QST to physical QST is approximately in the range of 70–289. Table 5 has shown that the characteristic time of mass diffusion (τ_d) ranges from 2.47 to 15.4 s within the investigated range of drop radius. In examining the ratios of physical QST to τ_d and chemical QST to τ_d, Fig. 11(b) depicts that the former is in the range of 0.12–0.43, whereas the latter is between 28 and 36. In other words, the physical QST is approximately in the same order of τ_d or less than it by an order of magnitude. Alternatively, the chemical QST is always larger than τ_d by over an order of magnitude.

With attention shifted to the absorption rate, Fig. 12 suggests that increasing drop size intensifies the physical absorption rate. This is attributed to the enlargements of droplet surface and terminal velocity, which are conducive to the transfer of SO_2 into the drop. Contrary to the behavior of physical absorption, an increase in drop size decreases the chemical absorption rate. This comes from the fact that the QST of chemical absorption is by far larger than that of physical absorption (Fig. 11(a)), even though the total uptake amount of SO_2 from chemical absorption is substantially larger than that from physical absorption (Fig. 6). Because of the difference between the physical absorption and the chemical one, when the ratio of chemical absorption rate (AR_{CA}) to physical one (AR_{PA}) is examined, the ratio has a pronounced trend to decrease with increasing drop size, as observed. However, the ratio is always larger than unity, revealing that the chemical absorption is faster than the physical one.

CONCLUSIONS

A simplified model of predicting SO_2 absorption processes by single freely falling raindrops under the combing effect of chemical dissociations and internal circulation has been developed in the present study. In the model, a modification factor α, the function of Reynolds number, is embedded into the formula of interfacial velocity based on the condition of creeping flow. With the simplified model (SM), only the drop phase is required to be solved for predicting the mass transport phenomena and the obtained results are close to those of the two-phase simulation method (TPSM), resulting from less than 4% of relative error. The analyses reveal that the characteristic time of mass diffusion is by far

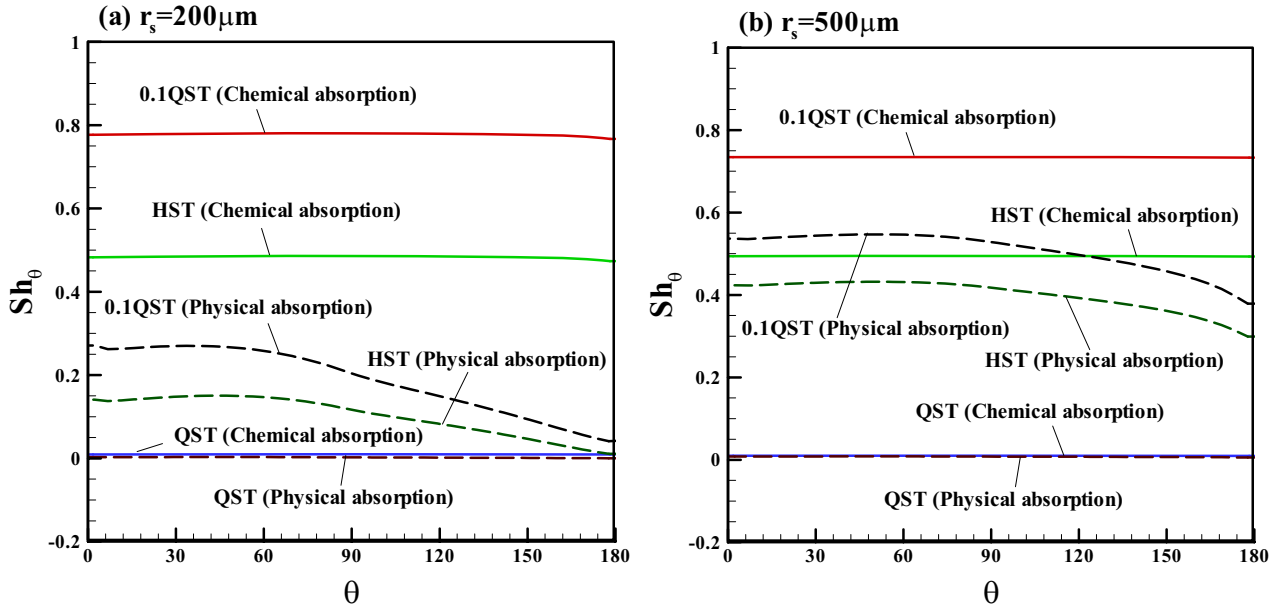

Fig. 10. Distributions of local Sherwood number at various absorption times with raindrop radii of (a) 200 and (b) 500 μm.

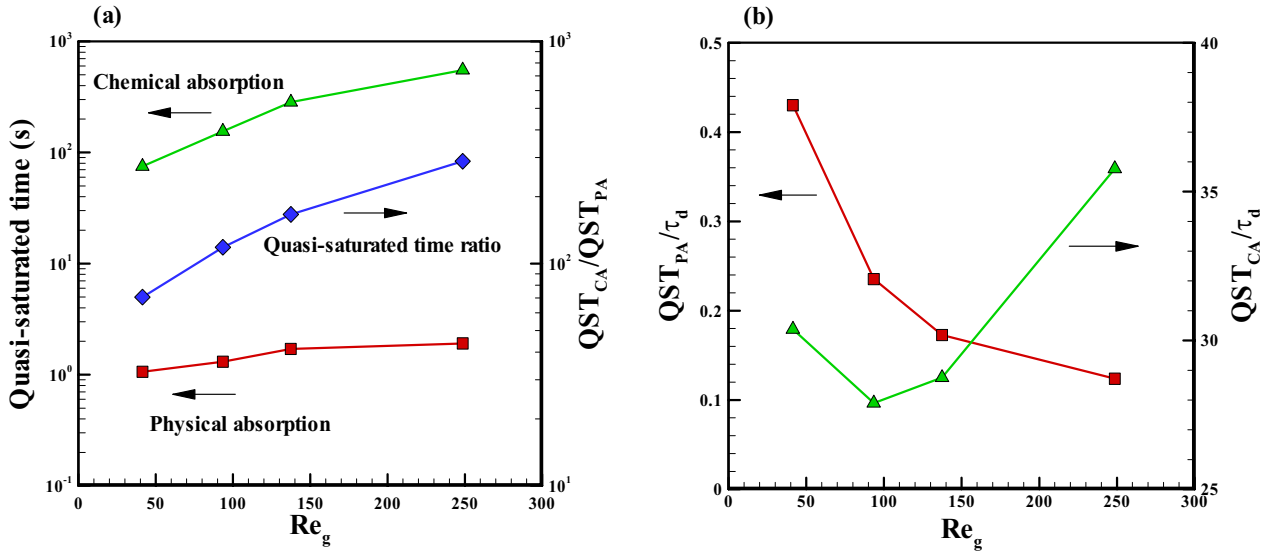

Fig. 11. Profiles of (a) QST of chemical absorption (CA) and physical absorption (PA) and their ratio as well as (b) the ratios of physical QST to characteristic time of diffusion and chemical QST to characteristic time of diffusion.

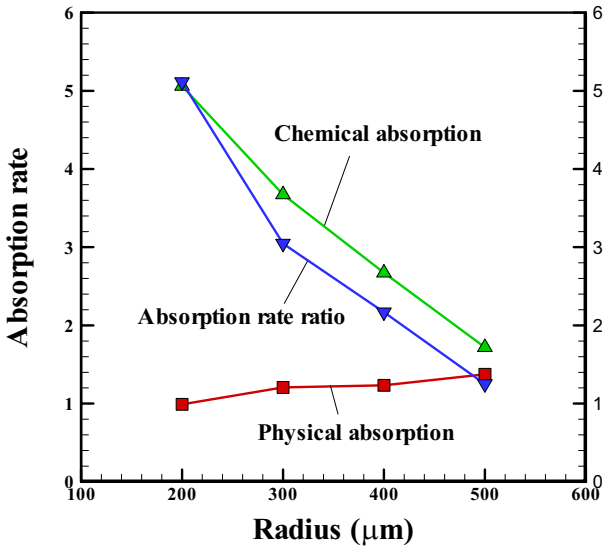

Fig. 12. Profiles of dimensionless physical and chemical absorption rates as well as their ratio.

longer than the others and the dissociation of sulfurous acid (H_2SO_3) dominates the species formation inside the raindrop. As a result, the absorption process of SO_2 is governed by the dissociation of H_2SO_3 and the chemical absorption period is much longer than the physical one. As a whole, for the raindrop radius in the range of 200–500 μm, the required chemical absorption time (i.e. the quasi-saturated time) ranges from 75 to 550 s which is larger than the physical one by the factors of 70–289. Meanwhile, the predictions suggest that the physical and chemical absorption periods are 0.12–0.43 and 28–36 folds of the characteristic time of mass diffusion, respectively. Eventually, it is found that increasing raindrop size enhances the physical absorption rate but a reverse trend is exhibited in the chemical absorption rate. It follows that the SO_2 uptake period has a significant effect on the absorption rate, even though the total SO_2 uptake amount is promoted notably in the chemical absorption process.

ACKNOWLEDGEMENTS

The authors gratefully acknowledge the financial support of the National Science Council, Taiwan, ROC, on this study.

NOMENCLATURE

C	Molar concentration (M)
D	Diffusion coefficient (m^2/s)
H	Henry's law constant (M/atm)
h^0	Standard-state enthalpy (J/kgmol)
k	Reaction rate constant (1/s)
K_{eq}	Equilibrium constant (M)
M_i	Molecular weight of species i (kg/kgmol)
m	Absorption amount
pH	pH value
p	Pressure (Pa)
r	Radial coordinate (m)
R	Universal gas constant (=8314.32 J/kgmol-K)
R_i	Reaction rate of species i ($kmol/m^3$-s)
Re	Reynolds number
$S(IV)$	Total dissolved sulfur
Sh	Sherwood number
s^0	Standard-state entropy (J/kgmol-K)
t	Time (s)
U_∞	Terminal velocity (m/s)
u	Axial velocity (m/s)
V	Velocity (m/s)

Greek letters

α	Modification factor
θ	Polar angle (°)

ρ	Density (kg/m^3)
υ	Radial velocity (m/s)
v	Stoichiometric coefficient
τ	Characteristic time (s)
μ	Viscosity (Pa s)

Subscript

atm	Atmosphere
aq	Aqueous phase
c	Convection
CA	Chemical absorption
d	Diffusion
eq	Equilibrium state
f	Forward direction in reaction
g	Gas phase
HSO_3^-	Hydrogen sulfite
H^+	Hydrogen ion
H_2O	Water
i	Species i
l	Liquid phase
min	Minimum
OH^-	Hydroxide ion
p	Phase equilibrium
qss	Quasi-saturated state
PA	Physical absorption
r	Reaction
s	Raindrop surface
$SO_2{\cdot}H_2O$	Sulfurous acid
SO_3^{2-}	Sulfite ion
SO2	Sulfur dioxide
t	Time

Superscripts

‘	Dimensionless scale

REFERENCES

Bhattacharyya, S. and Singh, A.K. (2010). Wake Flow and Heat Transfer Due to a Spherical Viscous Droplet. *Numer. Heat Transfer* 57: 138–158.

Chen, W.H. (2001a). Unsteady Absorption of Sulfur Dioxide by an Atmospheric Water Droplet with Internal Circulation. *Atmos. Environ.* 35: 2375–2393.

Chen, W.H. (2001b). Dynamics of Sulfur Dioxide Absorption in a Raindrop Falling at Terminal Velocity. *Atmos. Environ.* 35: 4777–4790.

Chen, W.H. (2002). An Analysis of Gas Absorption by a Liquid Aerosol in a Stationary Environment. *Atmos. Environ.* 36: 3671–3683.

Chen, W.H. (2006). Air Pollution Absorption by Single Moving Droplets with Drag Force at Moderate Reynolds Numbers. *Chem. Eng. Sci.* 61: 449–458.

Chen, W.H. and Lu, J.J. (2003). Microphysics of Atmospheric Carbon Dioxide Uptake by a Cloud Droplet Containing a Solid Nucleus. *J. Geophys. Res.* 108: 4470–4478.

Chen, W.H., Chiu, T.W., Hung, C.I. and Lin, M.R. (2009). Hysteresis and Reaction Characterization of Methane Catalytic Partial Oxidation on Rhodium Catalyst. *J. Power Sources* 194: 467–477.

Dong, C, Huang, K.L., Chen, C.W., Lee, C.W., Lin, H.Y. and Chen, C.F. (2002) Estimation of Air Pollutant Emission from Ship in Kaohsiung Harbor Area. *Aerosol Air Qual. Res.* 2: 31–40.

Elperin, T. and Fominykh, A. (2005). Conjugate Mass Transfer during Gas Absorption by Falling Liquid Droplet with Internal Circulation. *Atmos. Environ.* 39: 4575–4582.

Elperin, T., Fominykh, A. and Orenbakh, Z. (2007). Coupled Heat and Mass Transfer during Nonisothermal Absorption by Falling Droplet with Internal Circulation. *Int. J. Refrig* 30: 274–281.

Goncalves, F.L.T., Ramos, A.M., Freitas, S., Silva Dias, M.A. and Massambani, O. (2002). In-cloud and Below-cloud Numerical Simulation of Scavenging Processes at Serra Do Mar Region, SE Brazil. *Atmos. Environ.* 36: 5245–5255.

Hsieh, L.T., Wang, Y.F., Li, P. and Chen, K.C. (2011). Removal of Particle-bound Water-soluble Ions from Cooking Fume Using Bio-solution Wet Scrubber. *Aerosol Air Qual. Res.* 11: 508–518.

Hsu, C.T., Shih, S.M. and Chang, C.Y. (1994). Simulation of SO_2 Absorption by Falling Water Drops. *Can. J. Chem. Eng.* 72: 256–261.

Juncu, G. (1999). A Numerical Study of Steady Viscous Flow past a Fluid Sphere. *Int. J. Heat Fluid Flow* 20: 414–421.

Juncu, G. (2010). A Numerical Study of the Unsteady Heat/Mass Transfer Inside a Circulating Sphere. *Int. J. Heat Fluid Flow* 53: 3006–3012.

Leclair, B.P. and Hamielec, A.E. (1972). A Theoretical and Experimental Study of the Internal Circulation in Water Drops Falling at Terminal Velocity in Air. *J. Atmos. Sci.* 29: 728–740.

Lin, W.Y., Wu, Y.L., Yu, L.K., Wang, L.C. and Lu, X. (2010). The Emission and Distribution of PCDD/Fs in Municipal Solid Waste Incinerators and Coal-fired Power Plant. *Aerosol Air Qual. Res.* 10: 519–532.

Lu, H.H., Wu, T.C., Yang, Y.M. and Maa, J.R. (1998). Transient Heat and Mass Transfer in a Drop Experiencing Absorption with Internal Circulation. *Int. Commun. Heat Mass Transfer* 25: 1115–1126.

Mott, R.L. (1994). *Applied Fluid Mechanics*, 4th Edition. Prentice-Hall, NJ.

Oliver, D.L.R. and Chung, J.N. (1985). Steady Flows Inside and around a Fluid Spherical Droplet at Low Reynolds Numbers. *J. Fluid Mech.* 154: 215–230.

Oliver, D.L.R. and Chung, J.N. (1987). Flow about a Fluid Sphere at Low to Moderate Reynolds Numbers. *J. Fluid Mech.* 177: 1–18.

Patankar, S.V. (1980). *Numerical Heat Transfer and Fluid Flow*, Hemisphere, Washington, D.C.

Schwartz, S.E. and Freiberg, J.E. (1981a). Mass-transport Limitation to the Rate of Reaction of Gases in Liquid Droplets: Application to Oxidation of SO_2 in Aqueous Solutions. *Atmos. Environ.* 15: 1129–1144.

Schwartz, S.E. and Freiberg, J.E. (1981b). Oxidation of SO_2 in Aqueous Droplets: Mass-transport Limitation in Laboratory Studies and the Ambient Atmosphere. *Atmos. Environ.* 15: 1145–1154.

Seinfeld, J.H. (1986). *Atmospheric Chemistry and Physics*

of Air Pollution, Wiley, New York, p. 202–204.

Sirignano, W.A. (1999). *Fluid Dynamics and Transport of Droplets and Sprays*, Cambridge: Cambridge University Press, p. 264–265.

Sonntag, R.E., Borgnakke, C. and Van Wylen, G.J. (1994). *Fundamentals of Classical Thermodynamics*, Wiley, New York.

Sportisse, B. and du Bois, L. (2002). Numerical and Theoretical Investigation of a Simplified Model for the Parameterization of Below-cloud Scavenging by Falling Raindrops. *Atmos. Environ.* 36: 5719–5727.

Tanaka, Y. (2010). Water Dissociation Reaction Generated in an Ion Exchange Membrane. *J. Membr. Sci.* 350: 347–360.

Yan, Y.Y., Lai, H., Gentla, C.R. and Smith, J.M. (2002). Numerical Analysis of Fluid Flows Inside and around a Liquid Drop Using an Incorporation of Multi-block Iteration and Moving Mesh. *Chem. Eng. Res. Des.* 80: 325–331.

Received for review, August 13, 2011
Accepted, October 28, 2011